AB

KEK Preprint 95-171
December 1995
H

New Limits on the Masses of the Selectron and Photino

AMY Collaboration

CERN LIBRARIES, GENEVA
SCAN-9603058

Sw 96191

(Submitted to Physics Letters B)

National Laboratory for High Energy Physics, 1995

KEK Reports are available from:

Technical Information & Library
National Laboratory for High Energy Physics
1-1 Oho, Tsukuba-shi
Ibaraki-ken, 305
JAPAN

Phone: 0298-64-5136
Telex: 3652-534 (Domestic)
(0)3652-534 (International)
Fax: 0298-64-4604
Cable: KEK OHO
E-mail: Library@kekvax.kek.jp (Internet Address)

New limits on the masses of the selectron and photino

AMY Collaboration

Y. Sugimoto [a,1], K. Abe [a], Y. Fujii [a], S. Igarashi [a], Y. Kurihara [a], M.H. Lee [a], F. Liu [a], A. Maki [a], T. Nozaki [a], T. Omori [a], H. Sagawa [a], Y. Sakai [a], T. Sasaki [a], Y. Takaiwa [a], S. Terada [a], P. Kirk [b], T.J. Wang [c], A. Abashian [d], K. Gotow [d], L. Piilonen [d], S.K. Choi [e], C. Rosenfeld [f], L.Y. Zheng [f], R.E. Breedon [g], Winston Ko [g], R.L. Lander [g], J. Rowe [g], S. Kanda [h], S.L. Olsen [h], K. Ueno [h], F. Kajino [i], T. Aso [j], H. Miyata [j], K. Miyano [j], N. Nakajima [j], K. Ohkubo [j], M. Sato [j], M. Shirai [j], N. Takashimizu [j], Y. Yamashita [k], S. Schnetzer [l], S. Behari [m], H. Fujimoto [m], S. Kobayashi [m], A. Murakami [m], S.K. Sahu [m,p], M. Yang [m], J.S. Kang [n], D.Y. Kim [n], S.S. Myung [n], H.S. Ahn [o], S.K. Kim [o], S. Matsumoto [q]

[a] *KEK, National Laboratory for High Energy Physics, Ibaraki 305, Japan*
[b] *Louisiana State University, Baton Rouge, LA 70803, USA*
[c] *Institute of High Energy Physics, Beijing 100039, China*
[d] *Virginia Polytechnic Institute and State University, Blacksburg, VA 24061, USA*
[e] *Gyeongsang National University, Chinju 660-701, South Korea*
[f] *University of South Carolina, Columbia, SC 29208, USA*
[g] *University of California, Davis, CA 95616, USA*
[h] *University of Hawaii, Honolulu, HI 96822, USA*
[i] *Konan University, Kobe 658, Japan*
[j] *Niigata University, Niigata 950-21, Japan*
[k] *Nihon Dental College, Niigata 951, Japan*
[l] *Rutgers University, Piscataway, NJ 08854, USA*
[m] *Saga University, Saga 840, Japan*
[n] *Korea University, Seoul 136-701, South Korea*
[o] *Seoul National University, Seoul 151-742, South Korea*
[p] *National Taiwan University, Taipei 10764, China*
[q] *Chuo University, Tokyo 112, Japan*

(Submitted to Physics Letters B)

[1] E-mail address: sugimoto@kekvax.kek.jp

Abstract

A study of e^+e^- annihilations into final states containing a single energetic photon with no accompanying particles is made at a center of mass energy of 57.8 GeV. The measured cross section is consistent with expectations from standard model processes and is used to set limits on the masses of the scalar electron and photino particles predicted by supersymmetry theories. If the photino is assumed to be massless, the 90% confidence level lower limit on the mass of the degenerate scalar electron is 65.5 GeV. If the results of all the single photon experiments are combined, this lower limit increases to 79.3 GeV.

1 Introduction

Supersymmetry (SUSY) has been proposed as a solution to the gauge hierarchy problem [1, 2, 3]. SUSY theories predict that each known particle has a SUSY partner with a spin that differs by 1/2 and with a mass that is expected to be below $\mathcal{O}$(1 TeV). Experimental searches for SUSY particles have been performed by many groups, all with negative results.

An observation of the process $e^+e^- \to \tilde{\gamma}\tilde{\gamma}\gamma$ would provide evidence for the photino ($\tilde{\gamma}$) and the scalar electron ($\tilde{e}$), the SUSY partners of the photon and the electron. In this reaction, the scalar electron is exchanged in the t-channel and the cross section is a function of its mass as well as that of the photino [4, 5]. The scalar electron has two mass eigenstates, $\tilde{e_L}$ and $\tilde{e_R}$, corresponding to partner particles of the left- and right-handed electrons. In the experimental analysis reported here, the mass degenerate case ($m_{\tilde{e_L}} = m_{\tilde{e_R}}$) is considered and we assume that the photino is the lightest SUSY particle (LSP). In general, the LSP cannot decay due to R-parity conservation [6]. Furthermore, the interactions of the photino with the material of the detector is very weak because of the large mass of the scalar electron propagator [7]. As a consequence, the experimental signature of this reaction is a single detected photon and nothing else.

In the standard model, events with this single-photon signature can be produced by the radiative production of neutrino pairs, $e^+e^- \to \nu\bar{\nu}\gamma$. The cross section for this process depends on the number of neutrino generation N_ν, which has been measured by LEP experiments by the direct counting of radiative decays [8] and inferred from the invisible Z^0 width [9]. Both methods strongly support $N_\nu = 3$. The existence of SUSY particles would produce an excess in the number of single-photon events over the expectation from the standard model with $N_\nu = 3$.

The search reported here was performed using data collected with the AMY detector at TRISTAN at $\sqrt{s} = 57.8$ GeV. A data sample corresponding to a total integrated luminosity of 301 pb^{-1} was used. This sample was collected using four different configurations of the AMY detector; in the following discussion these four data subsets are referred to as data samples 1, 2, 3 and 4, with integrated luminosities of 55, 91, 56, and 99 pb^{-1}, respectively.

2 The AMY detector

Figure 1 shows the AMY detector [10]. Photons and electrons are detected by a cylindrical shower counter (SHC) [11] covering the polar angle (θ) range of $|\cos\theta| < 0.73$ with an energy resolution of $\sigma_E/E = 23\%/\sqrt{E} + 6\%$. We use the angular range of $|\cos\theta| < 0.7$ for the detection of the signal photon. The SHC is comprised of six modules in azimuthal angle (ϕ), each module consisting of 20 alternating layers of lead and proportional tube chambers with a total thickness of 14.4 radiation length (X_0). Each layer has orthogonal cathode strips for the measurement of the θ- and ϕ-coordinates of the shower centroid. The cathode strips of each four adjacent layers are summed, giving five samples along the development of the shower that we call *ganged*

layers. The measured positions of the shower centroids from the five ganged layers of ϕ- and θ-strips are fit to straight lines, providing a measurement of the photon's line of flight. The distances of closest approach between this line and the interaction point projected onto the R-ϕ ($d_{R\phi}$) and R-z (d_{Rz}) planes are calculated. The experimental resolutions for these distances are determined to be $\sigma_d = 3.1$ cm for 29 GeV electrons and $\sigma_d = 4.4$ cm for photons from $e^+e^-\gamma$ events, which have an energy spectrum that peaks at ~ 6 GeV. For data sample 4, SHC timing information with a resolution of $\sigma_t = 5$ ns is available.

In the forward-backward regions there are endcap shower counters (ESC) that extend the coverage down to $\theta = 10.8°$. The ESC consists of 15 alternating layers of lead and scintillator ($13.4X_0$ thick) with two planes of proportional tube chambers with θ- and ϕ-readout strips located at a depth of $4.5X_0$, near the position of the shower maximum. The calorimeter part of the ESC is segmented longitudinally into front and rear sections and azimuthally into 24 sectors. The coverage is further extended by the "small angle calorimeter" (SAC) down to $\theta = 3°$, and, for data samples 3 and 4, by the "beam pipe calorimeter" (BPC) down to $\theta = 1.9°$. The SAC and the BPC are lead-scintillator calorimeters with thicknesses of $17.2X_0$ and $17.9X_0$, respectively. The ESC can detect minimum ionizing particles, while the SAC and the BPC are sensitive only to high energy electromagnetic showering particles.

Charged particle tracks are detected in the vertex chamber (VTX), inner

tracking chamber (ITC) [12], and central drift chamber (CDC) [13]. Muon tracks are detected in four layers of muon chambers (MUO) located outside of the 1.7-m-thick iron return yoke of the 3-T superconducting solenoid [14]. In this analysis, information from the CDC and the MUO are used to veto events with charged particles.

Candidate single-photon events are triggered by either the total energy sum or by energy deposited in two adjacent ganged layers in the same ϕ section ($\Delta\phi = 30°$) of the SHC. The trigger threshold is ~ 7 GeV for data sample 1 and ~ 3.5 GeV for the other three data samples (see Table 1). Figure 2 shows the energy dependence of the trigger efficiency for these two different threshold levels.

3 Event selection

In the search for the single-photon events, there is a huge background coming from the radiative Bhabha process $e^+e^- \rightarrow e^+e^-\gamma$, where the e^+ and e^- escape into the beam pipe. This limits the search to events where the detected photon is above a minimum transverse energy, E_t, which depends on the minimum veto angle for electrons, θ_{veto}, as

$$E_t > \sqrt{s}\sin\theta_{veto}/(1+\sin\theta_{veto}). \quad (1)$$

In previous single-photon experiments [15], an E_t or, equivalently, x_t ($= E_t/E_{beam}$) cut is applied. In this analysis we apply a cut on the total photon energy x ($= E/E_{beam}$) rather than x_t, since this is found to be more effective

for rejecting cosmic ray background while still preserving good sensitivity for true single-photon events.

To select the single-photon event candidates, the following criteria are imposed:

(1) A single energy cluster is found in the SHC with the following properties:

- $E/E_{beam} > x_{min}$ and $|\cos(\theta)| < 0.7$, where $x_{min} = 0.175$ for data samples 1 and 2, and 0.125 for samples 3 and 4;
- a ϕ angle that is at least 1° away from the boundary of the SHC modules;
- no other SHC cluster with $E > 2$ GeV;
- no SHC cluster with $E > 0.7$ GeV opposite in ϕ to the signal cluster ($\Delta\phi > 175°$);
- the sum of the energy of other clusters with $E > 0.2$ GeV and either nearby ($\Delta\phi < 30°$) or opposite ($\Delta\phi > 150°$) in ϕ, is less than 1.5 GeV or the number of such clusters is less than 3; and
- no other cluster in the SHC with $E > 0.1$ GeV and collinear to the extrapolated line of the fitted trajectory of the signal cluster or collinear to the line connected between the signal cluster and a MUO track candidate if exists.

(2) No charged tracks in the CDC or MUO, as evidenced by:

- no reconstructed CDC track;

- no string of CDC hits consistent with a track pointing at the signal shower;
- no pair of MUO tracks candidates collinear to the SHC cluster; and
- less than two layers of MUO hits within 60 cm of the extrapolated line of the fitted trajectory of the SHC signal.

(3) The possibility of detector malfunction is avoided by requiring that the nominal chamber high voltage is on for 100% of the SHC and MUO modules and more than 50% of the CDC layers.

(4) Events with activity in the endcap detectors are vetoed if there is

- an energy cluster in the ESC with $E > 2$ GeV (either an electromagnetic or hadronic shower);
- an energy cluster in the ESC with energy deposit in both front and rear sections with $E > 0.2$ GeV (a minimum ionizing particle);
- an energy cluster in the ESC with $E > 0.1$ GeV at the edge ($\theta > 35°$) and ϕ angle opposite ($\Delta\phi > 175°$) to the signal cluster;
- an energy cluster in the SAC with $E > 10$ GeV; or
- an energy cluster in the BPC with $E > 20$ GeV.

(5) The lateral and longitudinal shower shape is required to be consistent with that of an electromagnetic shower caused by a photon coming from the interaction point.

(6) For data sample 4, the time of the SHC anode signal is required to occur within $\Delta t < 30$ ns of the beam crossing.

Events that satisfy all the above cuts are primarily due to cosmic rays that enter the detector through the region not covered by the MUO. Since the region $|\cos\theta| < 0.7$ is fully covered by the MUO, such events inevitably make showers that do not point to the interaction point, and cuts on the shower direction are effective for rejecting this background. For this, we use the normalized distances of the closest approach to the interaction point, $\delta_i = d_i/\sigma_i$, where d_i ($i = R\phi$ and Rz) are described above in section 2 and σ_i are the expected d_i resolutions for the event. The two-dimensional δ_i distribution for the events surviving cuts (1) through (6) is shown in Fig. 3(a); Fig. 3(b) shows the same distribution for photons from $e^+e^-\gamma$ events. We require

(7) $\sqrt{\delta^2_{R\phi} + \delta^2_{Rz}} < 2.5$.

Six events survive all cuts; these are evident in Fig. 3(a).

The efficiencies of the trigger and the selection cuts for each of the four data samples are obtained as functions of energy and $\cos\theta$ using event samples of QED processes. The trigger efficiency is determined using single-electron events from the $e^+e^-\gamma$ process triggered independently by a high energy electromagnetic shower in the ESC. The inefficiencies caused by vetos from accidental hits in the various detector components of the barrel (endcap) region are estimated using ESC (SHC) Bhabha events. In order to

determine the efficiencies of the cuts on the shape, timing and direction of the shower, photons from $e^+e^-\gamma$ and $\gamma\gamma$ processes are used. Event loss due to γ conversions in the material of the detector is determined using a Monte Carlo simulation. The overall efficiency $\bar{\epsilon}$ (the average efficiency weighted by the differential cross section for $e^+e^- \to \nu\bar{\nu}\gamma$) for each data sample is given, together with those from other single-photon experiments, in Table 2.

4 Background estimates

We considered backgrounds from cosmic rays and the processes $e^+e^- \to \nu\bar{\nu}\gamma$, $\gamma\gamma\gamma$, $e^+e^-\gamma$, $\mu^+\mu^-\gamma$, and $\tau^+\tau^-\gamma$.

To study the cosmic ray background, we use a cosmic ray data sample selected using the criteria (1)–(6) above, with the requirement on the CDC hit string or the SHC timing satisfying $\Delta t > 30$ ns, and some of the requirements for the shower shape loosened. The distributions of δ_i for the cosmic ray and the signal samples are compared. The region $2.5 < \sqrt{\delta^2_{R\phi} + \delta^2_{Rz}} < 5.0$, where there are 53 events in the signal sample, is used for normalization. The cosmic ray sample has 61 events in the normalization region and no events with $\sqrt{\delta^2_{R\phi} + \delta^2_{Rz}} < 2.5$. From this we conclude that the level of cosmic ray background in our signal sample is $0^{+1.6}_{-0}$ and contributions from this source are neglected in the following analysis.

The contribution from $\nu\bar{\nu}\gamma$ events is estimated using a Monte Carlo simulation based on the NNGG03 event generator [16]. This generator includes exact lowest order calculations for both W-exchange and Z^0-annihilation di-

agrams and higher order corrections for the Z^0 diagrams. We find that 7.2 events are expected from this process with $N_\nu = 3$.

There are two ways that $\gamma\gamma\gamma$ events can fake single-photon events: 1) one γ is detected by the SHC while the other two escape into the beam pipe; and 2) one γ is detected by the SHC, another escapes into the beam pipe, and the third is lost in the overlap region between the SHC and the ESC where the detector thickness is as low as $4X_0$. The level of background from these two cases is calculated using a Monte Carlo simulation using the BASES and SPRING [17] generator applied to the cross section calculation given in ref. [18]. It was found that the contribution from the first case is negligibly small while 0.8 events are expected from the second case.

The backgrounds from radiative charged lepton pair production are determined with a Monte Carlo simulation using the GRACE system [19], which includes exact tree-level calculations of the cross sections. The contribution from $e^+e^-\gamma$ events is found to be negligibly small due to the rather hermetic calorimetric coverage. For the $\mu^+\mu^-\gamma$ and $\tau^+\tau^-\gamma$ processes, however, it is found that there are contributions of 0.6 and 0.3 events, respectively, because of holes for minimum ionizing particles in the forward and backward regions ($\theta < 10.8°$).

In total, 8.9 ± 0.3 events are expected from the standard model processes. Here, the error includes Monte Carlo statistics (1.0–15.6% depending on the process), efficiency uncertainties (2.2%), and the luminosity measurement error (1.8%).

5 Results

As described in the previous sections, 6 events are selected as single-photon event candidates, whereas 8.9 events are expected from known standard model processes. Figure 4 shows the x distribution of the selected events together with the expectations for the standard model plus backgrounds.

Considering the $\nu\bar{\nu}\gamma$ process as a part of the signal, we can deduce the cross section for the single-photon production process to be 29^{+25}_{-18} fb for $x > 0.125$ and $|\cos\theta| < 0.7$. Here the error is dominated by the Poisson statistics of the 6 observed events and the error on our measurement of the cosmic ray background. This value is consistent with the expected $\nu\bar{\nu}\gamma$ cross section of 49 fb obtained from the NNGG03 calculation.

To set the limits on the SUSY particles, we follow the Bayesian approach [15, 20] that has been used by other single-photon experiments, and ignore the error on the estimated number of background events. The observation of 6 events when 8.9 are expected from known processes gives a 90% confidence level (CL) upper limit of 4.4 for the number of SUSY events. From this, 90% CL mass limits on the $m_{\tilde{e}}$–$m_{\tilde{\gamma}}$ plane are determined as shown in Fig. 5. The cross section for $e^+e^- \to \tilde{\gamma}\tilde{\gamma}\gamma$ was calculated using GRACE; we find the same results as given in ref. [5]. For a massless photino, the 90% CL lower limit for the degenerate scalar electron mass case is $m_{\tilde{e}} > 65.5$ GeV. If we change the expected number of events by $\pm 1\sigma$, this mass limit changes by ± 0.7 GeV.

We have combined our data with the results of other single-photon experiments at PEP, PETRA and TRISTAN [15]. The data used for the combined analysis are listed in Table 2. The 90% CL upper limit on the expected number of events from the SUSY process is 7.5 for 23.9 observed events with 28.2 expected from standard model processes, where the expected backgrounds from $\nu\bar{\nu}\gamma$ in other experiments are calculated using NNGG03. The corresponding 90% CL limit for the degenerate scalar electron mass for a massless photino is $m_{\tilde{e}} > 79.3$ GeV.

6 Summary

We have searched for SUSY particles by looking for an excess of single-photon events in e^+e^- collisions at $\sqrt{s} = 57.8$ GeV. In a data sample corresponding to an integrated luminosity of 301 pb^{-1} collected with the AMY detector, we observe 6 single-photon events, which is consistent with the expectation of 8.9 events from $\nu\bar{\nu}\gamma$ with $N_\nu = 3$ and other known backgrounds. No evidence for the existence of SUSY particles is found. The 90% CL limit on the mass of the degenerate scalar electron is $m_{\tilde{e}} > 65.5$ GeV for a massless photino. If we combine our result with other single-photon experiments, this limit is extended to $m_{\tilde{e}} > 79.3$ GeV.

Acknowledgement

We wish to thank J. Fujimoto, T. Kon, and R. Miquel for useful information and discussions on the Monte Carlo simulations. We thank the staff of TRISTAN for the excellent operation of the storage ring. We also thank the staffs of our home institutions for their strong support. This work has been supported by the Japan Ministry of Education, Science and Culture (Monbusho), the Japan Society for the Promotion of Science, the US Department of Energy, the US National Science Foundation, the Ministry of Education of Korea, and the Academia Sinica of the People's Republic of China.

References

[1] J. Wess and B. Zumino, Phys. Lett. 49B (1974) 52.

[2] C.H. Llewellyn Smith and G.G. Ross, Phys. Lett. 105B (1981) 38.

[3] S. Dimopoulos and H. Georgi, Phys. Lett. 117B (1982) 287.

[4] P. Fayet, Phys. Lett. 117B (1982) 460;
J. Ellis and J.S. Hagelin, Phys. Lett. 122B (1983) 303.

[5] K. Grassie and P.N. Pandita, Phys. Rev. D30 (1984) 22.

[6] P. Fayet, Phys. Lett. 69B (1977) 489;
G.R. Farrar and P. Fayet, Phys. Lett. 76B (1978) 575.

[7] P. Fayet, Phys. Lett. 86B (1979) 272.

[8] ALEPH Collab., D. Buskulic et al., Phys. Lett. B313 (1992) 520;
L3 Collab., O. Adriani et al., Phys. Lett. B292 (1992) 463;
OPAL Collab., M. Z. Akrawy et al., Z. Phys. C50 (1991) 373.

[9] The LEP Collaborations: ALEPH, DELPHI, L3, and OPAL, Phys. Lett. B276 (1992) 247.

[10] AMY Collab., T. Kumita et al., Phys. Rev. D42 (1990) 1339.

[11] A. Abashian et al., Nucl. Instrum. Methods A317 (1992) 75.

[12] M. Frautschi et al., Nucl. Instrum. Methods A307 (1991) 52.

[13] K. Ueno et al., Nucl. Instrum. Methods A323 (1992) 601.

[14] Y. Doi et al., Nucl. Instrum. Methods A274 (1989) 95.

[15] MAC Collab., W.T. Ford et al., Phys. Rev. D33 (1986) 3472;
H. Wu, Ph.D. Thesis, University of Hamburg (1986);
CELLO Collab., H.J. Behrend et al., Phys. Lett. B215 (1988) 186;
ASP Collab., C. Hearty et al., Phys. Rev. D39 (1989) 3207;
Y. Narita, Ph.D. Thesis, Tokyo Metropolitan University (1991);
VENUS Collab., N. Hosoda et al., Phys. Lett. B331 (1994) 211;
TOPAZ Collab., T. Abe et al., Phys. Lett. B361 (1995) 199.

[16] R. Miquel, C. Mana, and M. Martinez, Z. Phys. C48 (1990) 309.

[17] S. Kawabata, Comp. Phys. Comm. 41 (1986) 127.

[18] J. Fujimoto and M. Igarashi, Prog. Theor. Phys. 74 (1985) 791.

[19] T. Ishikawa et al., KEK Report 92-19, 1993, The GRACE manual Ver. 1.0.

[20] Particle Data Group, L. Montanet et al., Review of particle properties, Phys. Rev. D50 (1994) 1173.

[21] ALEPH Collab., D. Decamp et. al., Phys. Rept. 216 (1992) 253.

Figure captions

Figure 1. The AMY detector.

Figure 2. Trigger efficiencies as functions of the electron energy as measured by the CDC for two different run periods.

Figure 3. Two-dimensional distributions of the normalized distance of the closest approach δ_i to the interaction point projected onto the R–ϕ and R–z planes (a) for single-photon production candidates and (b) for photons from $e^+e^-\gamma$ events. The final shower direction cut is indicated by the dashed circle.

Figure 4. The x distribution for the selected events. The solid histogram is the Monte Carlo prediction for the sum of all background processes and the dashed histogram is for the $\nu\bar{\nu}\gamma$ process only.

Figure 5. The 90% CL lower limits on the masses of the scalar electron and the photino. The 90% CL limits from ASP, VENUS, and TOPAZ, and the 95% CL limit from ALEPH (ref. [21]) are also shown. The limit obtained by combining the results of all the single-photon experiments is shown as the dotted line.

Table 1: Summary of data samples.

Run period	$\int Ldt$	Trigger threshold	θ_{veto}	x_{min}	
1	55 pb^{-1}	7 GeV	3.0°	0.175	
2	91 pb^{-1}	3.5 GeV	3.0°	0.175	
3	56 pb^{-1}	3.5 GeV	1.9°	0.125	
4	99 pb^{-1}	3.5 GeV	1.9°	0.125	Δt cut

Table 2: Summary of single-photon experiments. The expected numbers of events for AMY, TOPAZ, and VENUS include background from sources other than the $\nu\bar{\nu}\gamma$ process. The cross section for $e^+e^- \to \nu\bar{\nu}\gamma$ integrated over the detector acceptance ($\sigma(\nu\bar{\nu}\gamma)$) is calculated using NNGG03; this results in some small changes in the expected number of events for some of the other experiments from their published values (given in parentheses).

	$\sqrt{s}$ (GeV)	$\int Ldt$ (pb^{-1})	$\bar{\epsilon}$	$\sigma(\nu\bar{\nu}\gamma)$ (fb)	Expected		Observed
AMY	57.8	55	0.44	34	1.0		0
		91	0.64	34	2.5		2
		56	0.58	49	2.0		2
		99	0.57	49	3.4		2
TOPAZ	58.0	213	0.27	52	5.8	(5.9)	5
VENUS	58.7	60	0.69	32	1.3	(1.3)	1
	58.0	164	0.57	36	7.5	(7.5)	8
CELLO	42.6	38	0.41	34	0.5	(0.7)	1.3
	35.0	85	0.50	23	1.0	(1.2)	
MARK J	39.0	36	0.57	15	0.3	(0.4)	0
ASP	29.0	110	0.61	32	2.1	(2.6)	1.6
MAC	29.0	36	0.74	3	0.1	(0.1)	0
		80	0.62	11	0.5	(0.6)	1
		61	0.69	8	0.3	(0.4)	0
Total					28.2		23.9

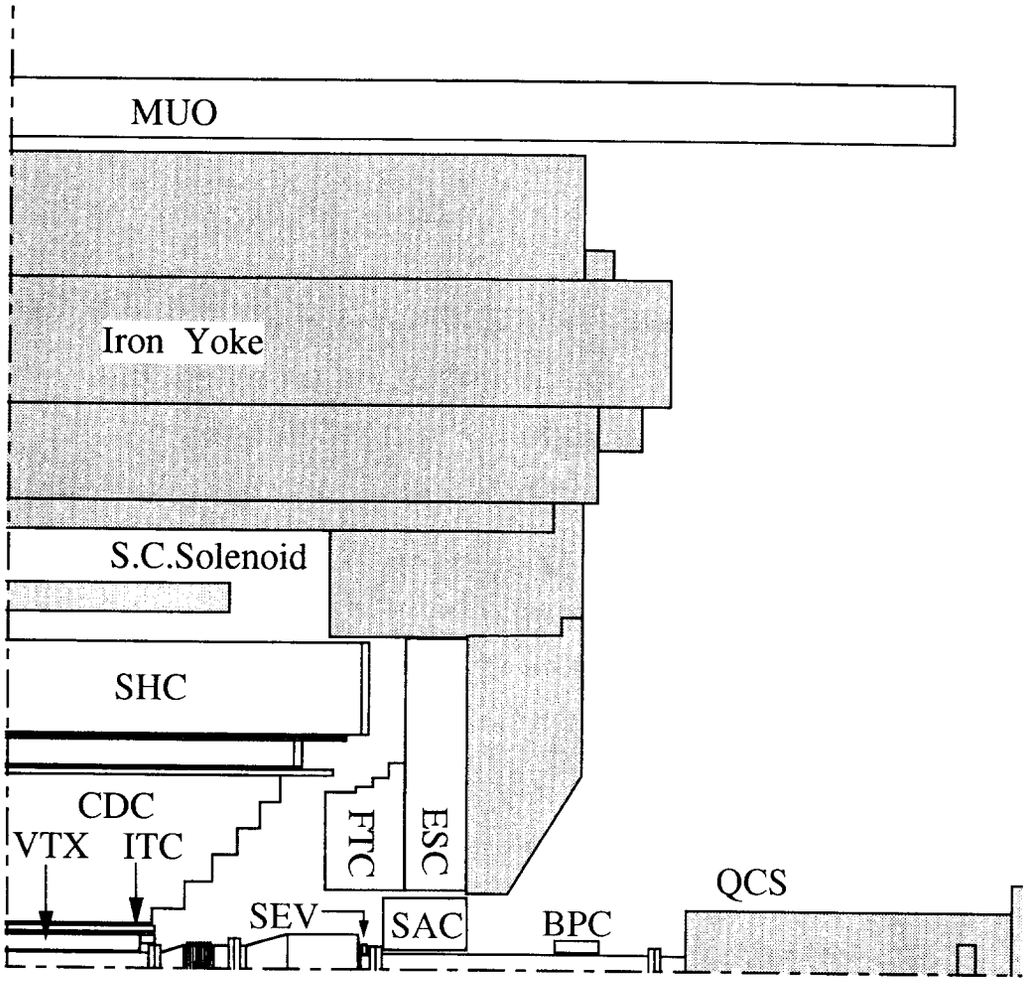

Figure 1:

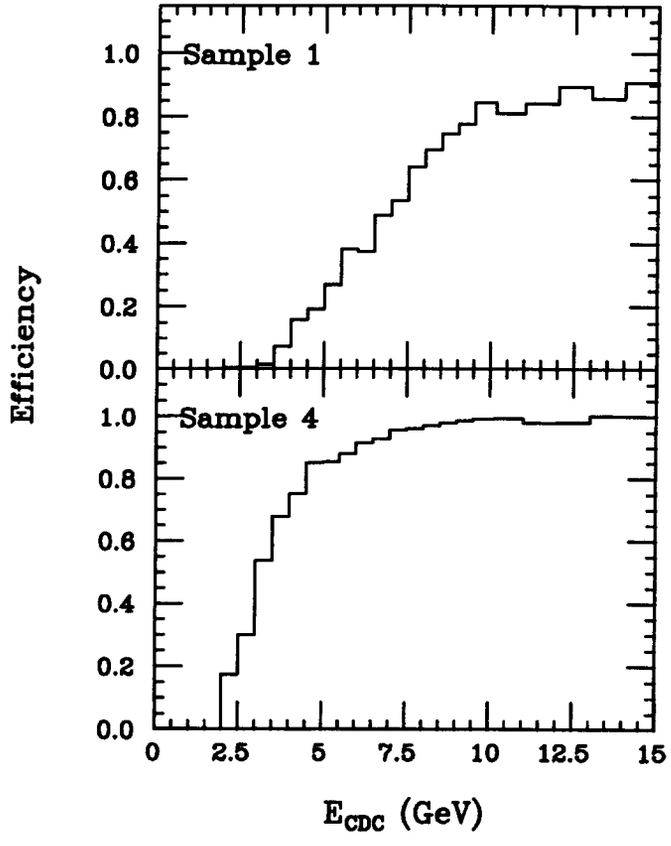

Figure 2:

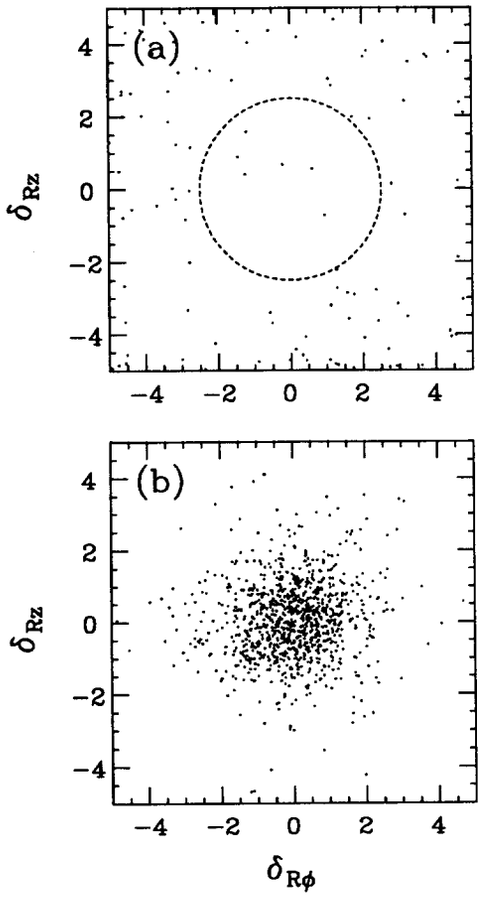

Figure 3:

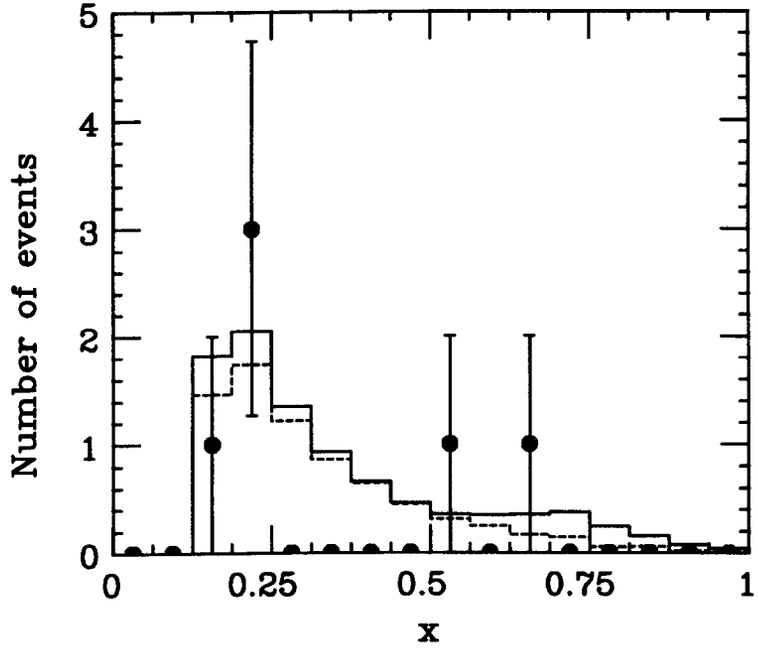

Figure 4:

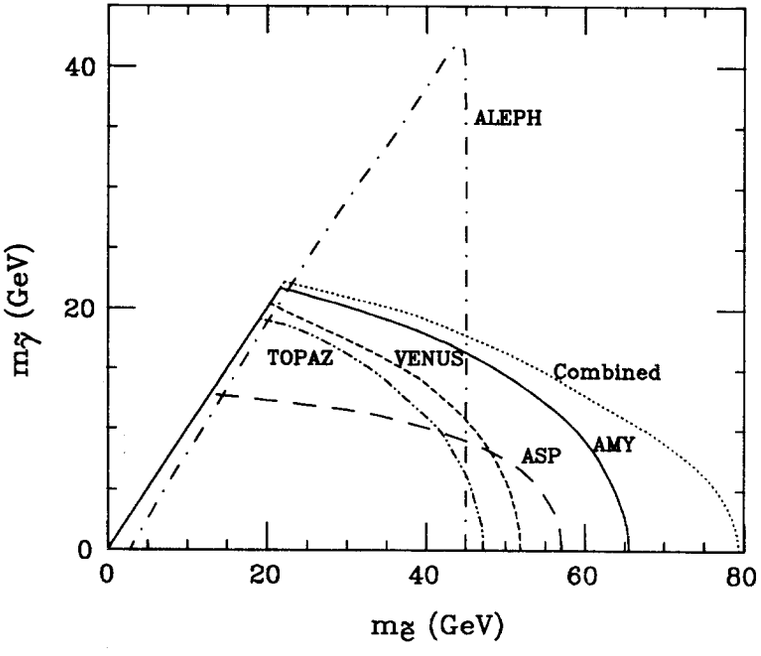
40
20
0
0
20
40
60
80
mγ̃ (GeV)
mg̃ (GeV)
ALEPH
TOPAZ
VENUS
Combined
ASP
AMY

Figure 5: